Experimental demonstration of deflection angle tuning in unidirectional fishnet metamaterials at millimeter-waves

Rodríguez-Ulibarri, P.; Pacheco-Peña, V.; Navarro-Cia, Miguel; Serebryannikov, A. E.; Beruete, M.

DOI:
10.1063/1.4908260

Document Version
Publisher's PDF, also known as Version of record

Citation for published version (Harvard):
Rodríguez-Ulibarri, P, Pacheco-Peña, V, Navarro-Cia, M, Serebryannikov, AE & Beruete, M 2015, 'Experimental demonstration of deflection angle tuning in unidirectional fishnet metamaterials at millimeter-waves', Applied Physics Letters, vol. 106, no. 6, 061109. https://doi.org/10.1063/1.4908260

AIP | Applied Physics Letters

Experimental demonstration of deflection angle tuning in unidirectional fishnet metamaterials at millimeter-waves

P. Rodríguez-Ulibarri, V. Pacheco-Peña, M. Navarro-Cía, A. E. Serebryannikov, and M. Beruete

Citation: Applied Physics Letters **106**, 061109 (2015); doi: 10.1063/1.4908260
View online: http://dx.doi.org/10.1063/1.4908260
View Table of Contents: http://scitation.aip.org/content/aip/journal/apl/106/6?ver=pdfcov
Published by the AIP Publishing

Experimental demonstration of deflection angle tuning in unidirectional fishnet metamaterials at millimeter-waves

P. Rodríguez-Ulibarri,[1,a)] V. Pacheco-Peña,[1,b)] M. Navarro-Cía,[2,3,4,c)]
A. E. Serebryannikov,[5,d)] and M. Beruete[1,e)]
[1]*Antennas Group - TERALAB, Universidad Pública de Navarra, 31006 Pamplona, Spain*
[2]*Optical and Semiconductor Devices Group, Department of Electrical and Electronic Engineering, Imperial College London, London SW7 2BT, United Kingdom*
[3]*Centre for Plasmonics and Metamaterials, Imperial College London, London SW7 2AZ, United Kingdom*
[4]*Centre for Terahertz Science and Engineering, Imperial College London, London SW7 2AZ, United Kingdom*
[5]*Faculty of Physics, Adam Mickiewicz University, Poznań 61-614, Poland*

(Received 23 December 2014; accepted 4 February 2015; published online 11 February 2015)

Asymmetric transmission enables high forward-to-backward transmission contrast in the Lorentz reciprocal framework, so that it is envisioned to be a backbone of future practical devices with strong directional selectivity. In this letter, we experimentally demonstrate efficient tuning and sign-switching capabilities of the deflection angle by varying the incidence angle and/or frequency in the unidirectional regime of a compact and simple structure comprising a stack of a fishnet metamaterial and a dielectric grating. The entire device operates at frequencies ranging from 45 to 75 GHz and has a total thickness of $0.77\lambda_0$ at 60 GHz. © *2015 AIP Publishing LLC*.
[http://dx.doi.org/10.1063/1.4908260]

Devices enabling strong directional selectivity like isolators and circulators play a very important role in modern microwave to optical technology. Simultaneous strong forward transmission and inhibited backward transmission are achievable in a two-port system in the nonreciprocal framework and, thus, commonly require components based on magnetic field biased ferrites.[1,2] Lately, alternative approaches to non-reciprocity have been suggested that do not require biased ferrites, e.g., see Ref. 3. Recently, the interest in direction selective devices realizable in the Lorentz reciprocal regime is growing, because they promise to open new frontiers for practical applications. Reciprocal devices are passive and comparatively simpler, although they cannot reproduce the operation regimes and functionalities typically achievable in nonreciprocal devices. In such reciprocal devices, the direction selective regimes require breaking spatial inversion symmetry.

Non-symmetric reciprocal finite-thickness/-size structures enable asymmetric transmission that can result in a strong forward-to-backward transmission contrast.[4,5] In the limiting case, the backward transmission vanishes leading to the most interesting—unidirectional—regime. Different strategies have been proposed, including those based on higher diffraction orders,[6–11] polarization conversion,[12,13] and wave manipulation in prism-like structures.[14,15] For the first and second ones, asymmetry in transmission is achieved due to the use of different transmission channels that are open for each of the two opposite illumination directions at fixed frequency. The third one can be achieved just owing to the effect of inclining interface(s), without a formal addition of new channels. Asymmetric excitation of higher diffraction orders can be simply enabled in various volumetric and ultrathin structures by loading one of the interfaces with a grating-like structure. This strategy has successfully been realized in non-symmetric structures based on photonic crystals,[6–9,16] fishnet,[17] and multilayer metamaterials,[18] thin metallic gratings with slits,[10,19] and simple one- and two-fraction gratings that contain Drude metals[7] or polar dielectrics.[20] Experimental results have been reported for acoustic,[9] microwave, [16,17] terahertz,[10] and optical[15,18] regimes. The simplest case when unidirectional transmission can be obtained is associated with isotropic type dispersion with circular equifrequency contours (EFCs) narrower than in air.[7,8,16,17,20,21] Clearly, it can also be possible when EFCs have another shape provided they are still narrower than in air.

Following the strategy based on higher diffraction orders, we present here experimental results on tuning and sign-switching of deflection angle that is obtained in a unidirectional structure based on a fishnet metamaterial[22] with a dielectric grating at one of the interfaces. The main goal is to experimentally validate our previous theoretical findings related to possible co-existence of unidirectionality and tunability of deflection angle when EFCs are narrower than in air.[21] At the same time, we extend our previous results of Ref. 17, where unidirectional operation was only demonstrated at normal deflection angle. The fishnet operates at the extraordinary transmission (ET) resonance, while the dielectric grating enables the excitation of higher diffraction orders. The total thickness of the device is reduced significantly to about $0.77\lambda_0$ (at 60 GHz) which is unachievable with photonic crystals.[8,9,16] This feature entails great benefits in terms of integration, avoiding bulky structures. Furthermore, the engineered structure provides unidirectional transmission in wide frequency and angular ranges and simultaneously enables tuning and sign-switching of the

[a)]Electronic mail: pablo.rodriguez@unavarra.es
[b)]Electronic mail: victor.pacheco@unavarra.es
[c)]Electronic mail: m.navarro@imperial.ac.uk
[d)]Electronic mail: andser@amu.edu.pl
[e)]Electronic mail: miguel.beruete@unavarra.es

output deflection angle of a single outgoing beam by properly changing the angle of incidence and/or frequency.

The structure under study is a four-layered fishnet combined with a dielectric grating, see Fig. 1(b) insets. Each hole array has the following nominal structural parameters: in-plane periods $d_x = 3.4$ mm, $d_y = 1.5$ mm; aperture diameter $a = 1.2$ mm; metal thickness, $t = 35$ μm; substrate has permittivity $\varepsilon_s = 2.43$; and thickness $h = 0.49$ mm. The grating parameters are: bar's thickness $a_z = 1.27$ mm, bar's height $a_x = 5.68$ mm, permittivity $\varepsilon_g = 10.2$, which correspond to ARLON AD 1000 commercial substrate material, and grating period $L = 3d_x$. The total thickness of the structure (including the grating) is 3.86 mm. The prototype was fabricated via milling machining and the four hole array layers as well as the grating were stacked together by mechanical pressure and attached by using dielectric screws situated close to the edges of the wafers.

Figure 1(a) shows a schematic of the experimental setup. In turn, Fig. 1(b) shows a picture of the manufactured prototype together with the sample holder placed on top of the rotating positioner. In the insets of the figure, details about the grating arrangement and fishnet metamaterial structural parameters are provided. The experimental characterization was performed by using an AB-Millimetre™ vector network analyzer operating at the V-band of the millimeter-wave spectrum. A metallic bench was used wherein the transmitter (TX) and receiver (RX) antennas, positioners, and sample were mounted. To correctly excite the ET resonance related to the four layered fishnet metamaterial, TX and RX antennas were horizontally polarized so that the electric field was parallel to the hole array long in-plane period, i.e., to the x direction. The RX antenna, the sample holder, and a manual rotating positioner were

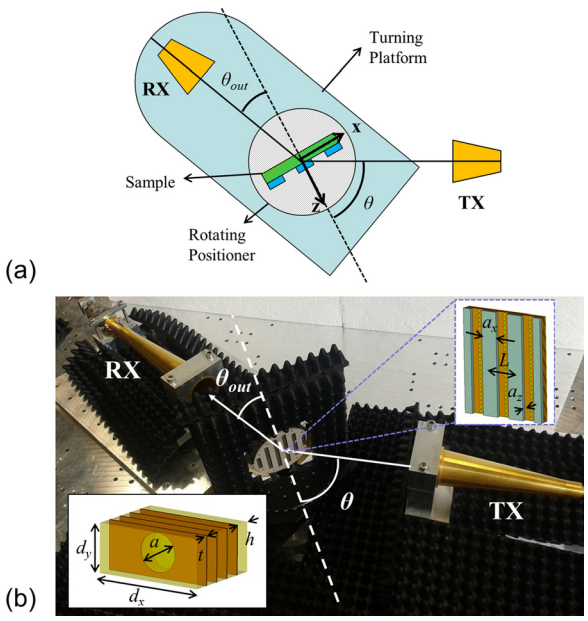

FIG. 1. (a) Schematic of the experimental setup in case of configuration for positive deflection angle measurement. (b) Setup picture. TX and RX antennas are shown. Sample holder mounted on top of the rotating positioner together with its normal axis and input and output angles are depicted. Top inset: Grating structure characteristics. Bottom inset: Fishnet unit cell dimensions.

situated on top of an electronically controlled turning platform with a very accurate control over both input and output angles contributing to the overall precision of the measurements. The angle of incidence (input angle) was varied with the electronically controlled turning platform. Positive/negative deflection angles were recorded by rotating the sample clockwise/counterclockwise with the manual rotating positioner.

Given the distances between horn antennas and the sample, a near-field experiment (i.e., $d_i < 2D_a^2/\lambda$, where d_i is the distance between the TX or RX and the sample, and D_a is the diameter of the antenna horn) was carried out. With this configuration, the Gaussian beam impinges on the sample with a beam radius of 18.3, 16.9, and 16.2 mm at 45, 60, and 75 GHz which represents the 58.19%, 53.7%, and 51.48% of the sample radius (31 mm), respectively. Thus, undesired reflection and diffraction effects due to interference with the sample holder, positioners, etc., are minimized at the expense of a non-uniform sample illumination. Then, some deviation from the theoretical/numerical expectations is envisaged. Another reason for potential disagreements is the presence of air gaps between fishnet layers.[23] These air gaps are expected to decrease the effective permittivity of the whole structure, blueshifting the response of the structure and somehow deprecating its performance. In fact, simulations with air gaps between the structure layers have been run[24] denoting an obvious blueshift in the operation frequency compared to the numerical results presented in Ref. 21.

To experimentally demonstrate the deflection angle tuning and, in particular, sign-switching, we selected five output deflection angles ($\theta_{out} = -10°$, $-5°$, $0°$, $5°$, $10°$) and varied the incidence angle θ from 10° to 80° with a step of 1° within a frequency span from 45 to 75 GHz (i.e., V-band). To confirm unidirectionality, both grating and non-grating sides were illuminated in successive experiments. From now on, forward/backward transmission will correspond to grating side/non-grating side illumination. Figure 2 shows forward transmission and forward-to-backward transmission contrast obtained at $\theta_{out} = +5°$ and $-5°$. Additionally, isolines of the output angle for diffraction orders $m = -1$ (white lines in the lower-half plot) and $m = -2$ (white lines in the upper-half plot) are superimposed. These lines are calculated by using the well-known grating formula:

$$\sin\phi_m = \sin\theta + 2\pi m/kL, \tag{1}$$

where ϕ_m is the output angle for diffraction order m, θ is the angle of incidence, L is the grating period, and k is the wavenumber.

Let us focus on forward transmission plots depicted in Fig. 2. A high transmission region is observed between 55 and 70 GHz for input angles between 40° and 20°. Comparing with the ϕ_{-1} isolines, one may assign this region to the first diffraction order ($m = -1$) excited by the grating. The second high transmission region is recorded between 60 and 70 GHz (slightly broken at ~65 GHz for $\theta_{out} = +5°$) and $\theta = 50°$–$70°$. This frequency/angle of incidence (f-θ) region is linked to the $m = -2$ diffraction order as it is corroborated by the ϕ_{-2} isolines. Much lower transmission levels appear

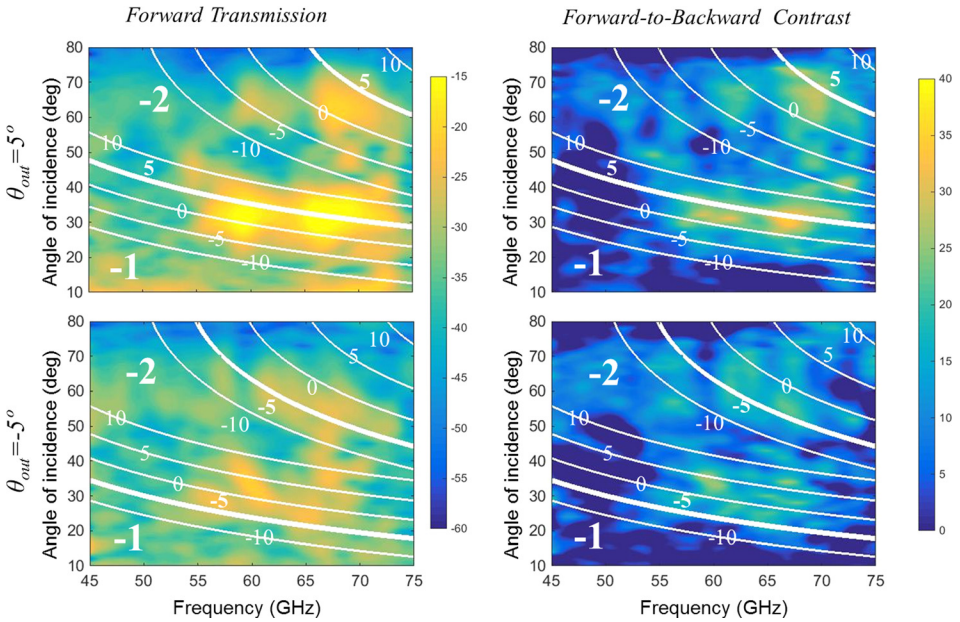

FIG. 2. Maps corresponding to $\theta_{out}=+5°$ (top), $\theta_{out}=-5°$ (bottom) deflection angle for forward transmission (left), and forward-to-backward transmission contrast (right) in (f-θ)-plane in dB scale; white lines—isolines for ϕ_{-1} and ϕ_{-2} obtained from Eq. (1); small numbers near isolines—values of ϕ_{-1} and ϕ_{-2} in degree; large numbers refer to a group of isolines associated with the m-diffraction order.

at backward illumination in this f-θ region, demonstrating a clear contrast between forward and backward transmission (see right panels of Fig. 2). Indeed, the contrast plots show differences up to 35 dB for $m=-1$ and about 30 dB for $m=-2$ for $\theta_{out}=+5°$. It can be noticed that high transmission is also found at f-θ regions that according to the predictions based on the ϕ_{-1} and ϕ_{-2} isolines, correspond to different output angles. Ideally, i.e., with infinitely directive receivers, we would collect uniquely the energy at a single output angle. Nevertheless, antennas have a finite effective area and they receive power arriving at different directions within a narrow angular interval, rather than from a single direction. Furthermore, as we are operating in near field, we can expect coupling within a relatively wide angular interval. In fact, high transmission appears at f-θ regions corresponding to output angles $\theta_{out}\approx\phi_{-1}\pm5°$. Summing up, unidirectionality is clearly observed at $\theta_{out}=+5°$ deflection angle for two different f-θ regions being more evident at the $m=-1$ diffraction order operation regime. However, for $\theta_{out}=-5°$ the contrast between forward and backward transmission is not so clear when dealing with the $m=-1$ diffraction order. In this case, the theory anticipates that the unidirectional operation regime of this structure should occur at lower incidence angles and/or lower frequencies.[21] If we observe $\theta_{out}=-5°$ scenario at forward transmission, there is some energy linked to diffraction order $m=-1$ at 60 GHz-35° that, according to the grating formula, corresponds to $\theta_{out}=0°, +5°$: there are hot-spots that coincide with the lines labeled by 0 and 5. This feature also appears in the forward-to-backward transmission contrast plot and dominates over the contrast observed at f-$\theta=56$ GHz–28° which corresponds to $\theta_{out}=-5°$. On the other hand, the agreement between the hot-spot and the $\theta_{out}=-5°$ isoline is better for the $m=-2$ band. Forward-to-backward contrast levels of 25 dB are achieved at f-$\theta=65$ GHz–55°. Although high transmission bands appear in the spectra related to diffraction order $m=-1$ (e.g., at f-$\theta=55$ GHz–25°g), forward-to-backward transmission contrast cannot be clearly identified as it can be seen at lower panels of Fig. 2. Numerical calculations considering material absorption have been performed (not shown here) indicating the same trend, i.e., negative deflection cases display lower levels of forward transmission and forward-to-backward transmission contrast. This suggests that for negative deflection cases losses have more influence and the expected performance of the device might be no longer obtained.

To provide additional evidences of the tuning and sign-switching capabilities for the deflection angle, another representation of the results is given next in terms of forward-to-forward transmission contrast maps for different output (deflection) angles, i.e., $\mathrm{FT}(\theta_{out}=\theta_1)/\mathrm{FT}(\theta_{out}=\theta_2)$, see Fig. 3. For consistency purposes, we always keep $\theta_1>0$

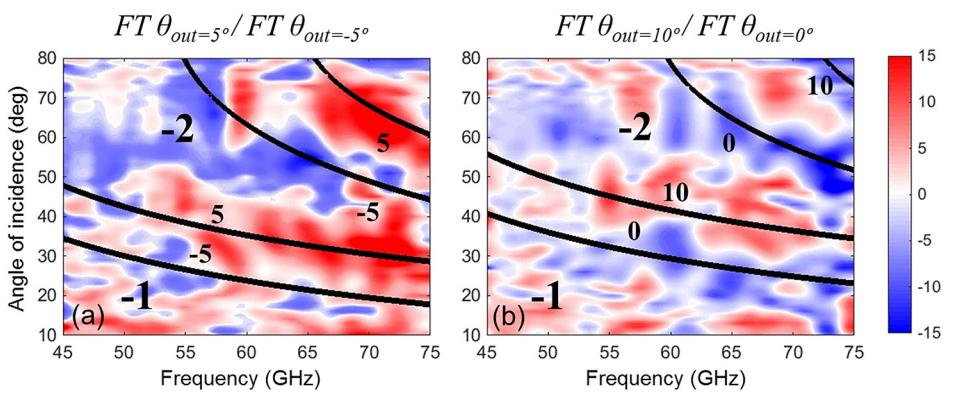

FIG. 3. Maps of forward-to-forward transmission contrast between $\theta_{out}=+5°$ and $\theta_{out}=-5°$ (left) and $\theta_{out}=+10°$ and $\theta_{out}=0°$ (right) deflection angle in (f-θ)-plane in dB scale; black lines—isolines for ϕ_{-1} and ϕ_{-2} obtained from Eq. (1); small numbers near isolines—values of ϕ_{-1} and ϕ_{-2} in degree; large numbers refer to a group of isolines connected with the m-diffraction order.

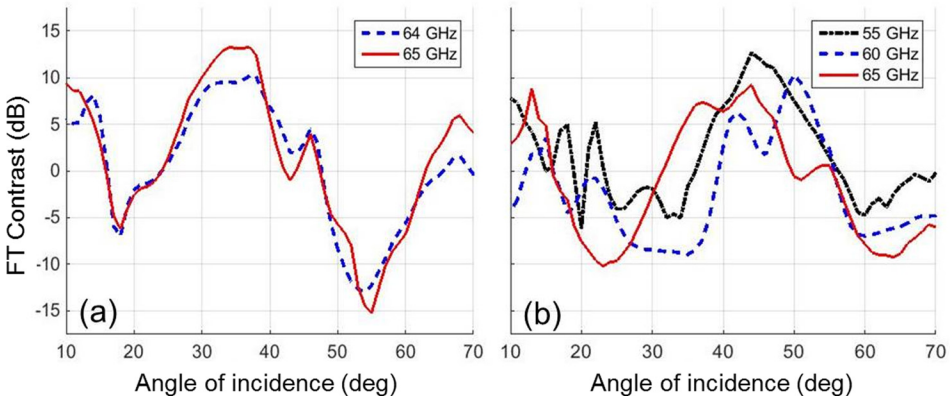

FIG. 4. Forward-to-forward transmission contrast versus angle of incidence at different frequencies: (a) FT ($\theta_{out} = +5$)/FT ($\theta_{out} = -5$); (b) FT ($\theta_{out} = +10$)/FT ($\theta_{out} = 0$).

and $\theta_2 \leq 0$. With this ratio, positive/negative contrast values may account for positive/negative deflection. Sign-switching can be safely claimed if a great excursion from positive to negative contrast values, or vice versa, is observed at a fixed frequency. In other words, different ranges of the incidence angle may correspond to different deflection angle sign of the outgoing wave in this case. As an example, Fig. 3 shows forward-to-forward transmission contrast between $\theta_{out} = +5°$ and $\theta_{out} = -5°$, and between $\theta_{out} = 10°$ and $\theta_{out} = 0°$ for demonstration of sign-switching (first case) and tuning (both cases) of the deflection angle. In particular, sign-switching can be observed around 65 GHz [see Fig. 3(a)], where dark blue areas correspond to negative deflection and red ones to positive deflection. By varying the incidence angle, one is able to steer the output beam, i.e., vary θ_{out} from negative to positive values and vice versa. Transition from positive to negative values of the contrast when moving along the incidence angle axis at fixed frequency indicates transition from the positive to the negative deflection angle. Similarly, tuning of the deflection angle from normal to 10° with frequency and input angle is also observed [see Fig. 3(b)]. In this case, negative values of the contrast correspond to the normal direction output, while its positive values do it for 10°. It can be noticed that both $m = -1$ and $m = -2$ diffraction orders can be simultaneously employed for deflection angle tuning.

Figure 4 presents cuts of Fig. 3 for the selected cases, in order to reinforce the previous discussion and demonstrate the choice of most desirable operation regimes. The cuts represent dependencies of the forward-to-forward transmission contrast on angle of incidence, at fixed frequency. In particular, at 65 GHz, positive deflection is observed at 35° and 40° due to the order $m = -1$ in Figs. 4(a) and 4(b), respectively. In Fig. 4(a), it is switched to negative deflection by varying the incidence angle up to 55°. Here, transmission is connected with the order $m = -2$. Similar behavior is also observed in the 64 GHz cut. In Fig. 4(b), a slightly different angle variation results in the change from positive deflection at nearly 40° ($m = -1$) to a deflection-free case near 60° ($m = -2$). Two more frequency cuts, at 55 and 60 GHz, are plotted showing similar results. Finally, one may find another switching scenario at 64 GHz by using $\theta_{out} = +10°$ and $\theta_{out} = -5°$ and changing the incidence angle from 38° to 51° (see supplementary material[24]). In order to prove that the selected cases are appropriate for tunable deflection in the unidirectional transmission regime, one should check whether the forward-to-backward transmission contrast is high enough. To do this, we used the cuts that are similar to those in Fig. 4 but are plotted for the forward-to-backward transmission contrast in Fig. 2 (see supplementary material[24]). Besides, one should check whether transmission levels, at least for the forward transmission, are far from the noise floor of the instrumentation. These restrictions have been considered in the context of the obtained experimental results. This consideration led us to the positive conclusion regarding the cases selected by using the results in Fig. 4.

To sum up, experimental results for a compact diffraction inspired unidirectional structure have been presented in the V-band of the millimeter-wave range. They confirm the possibility of tunable deflection in the unidirectional regime that has earlier been suggested in the framework of the theory developed for the structures with equifrequency dispersion contours narrower than in air. Forward-to-backward transmission contrast levels up to 35 dB have been obtained for the best performances. Tuning of the output deflection angle from positive values to zero (i.e., normal direction) and from positive to negative values has been observed in the unidirectional regime when varying the incidence angle at a fixed frequency and vice versa. Therefore, the experimental demonstration conducted in this letter would lead us to the design of new devices such as tunable deflectors, angular filters, and diodelike devices.

In memoriam Professor Mario Sorolla.

This work was sponsored by the Spanish Government and European Union funds under contracts Consolider "Engineering Metamaterials" CSD2008-00066 and TEC2011-28664-C02-01. P.R.-U. is sponsored by Public University of Navarra via a predoctoral scholarship. V.P.-P. is sponsored by Spanish Ministerio de Educación, Cultura y Deporte under Grant No. FPU AP-2012-3796. M.B. is sponsored by the Spanish Government via RYC-2011-08221. M.N.-C. is supported by the Imperial College Junior Research Fellowship. Contribution of AES was partially supported by ESF within the activity entitled "New Frontiers in Millimetre/Sub-Millimetre Waves Integrated Dielectric Focusing Systems."

[1]B. Lax and K. J. Button, *Microwave Ferrites and Ferrimagnetics* (McGraw-Hill, New York, 1962).
[2]J. D. Adam, L. E. Davis, G. F. Dionne, E. F. Schloemann, and S. N. Stitzer, IEEE Trans. Microwave Theory Tech. **50**, 721 (2002).

[3]T. Kodera, D. L. Sounas, and C. Caloz, IEEE Trans. Microwave Theory Tech. **61**, 1030 (2013).
[4]M. J. Lockyear, A. P. Hibbins, K. R. White, and J. R. Sambles, Phys. Rev. E **74**, 056611 (2006).
[5]A. E. Serebryannikov, T. Magath, K. Schuenemann, and O. Y. Vasylchenko, Phys. Rev. B **73**, 115111 (2006).
[6]A. Mandatori, M. Bertolotti, and C. Sibilia, J. Opt. Soc. Am. B **24**, 685 (2007).
[7]A. E. Serebryannikov and E. Ozbay, Opt. Express **17**, 13335 (2009).
[8]A. E. Serebryannikov, Phys. Rev. B **80**, 155117 (2009).
[9]X. F. Li, X. Ni, L. Feng, M. H. Lu, C. He, and Y.-F. Chen, Phys. Rev. Lett. **106**, 084301 (2011).
[10]M. Stolarek, D. Yavorskiy, R. Kotyński, C. J. Zapata-Rodríguez, J. Lusakowski, and T. Szoplik, Opt. Lett. **38**, 839 (2013).
[11]J. Xu, C. Cheng, M. Kang, Z. Zheng, Y. X. Fan, and H. T. Wan, Opt. Lett. **36**, 1905 (2011).
[12]E. Plum, V. A. Fedotov, and N. I. Zheludev, Appl. Phys. Lett. **94**, 131901 (2009).
[13]J. Shi, X. Liu, S. Yu, T. Vu, Z. Zhu, H. F. Ma, and T. J. Cui, Appl. Phys. Lett. **102**, 191905 (2013).
[14]A. Cicek, O. A. Kaya, and B. Ulug, Appl. Phys. Lett. **100**, 111905 (2012).
[15]C. Wang, X. L. Zhong, and Z. Y. Li, Sci. Reps. **2**, 674 (2012).
[16]A. O. Cakmak, E. Colak, A. E. Serebryannikov, and E. Ozbay, Opt. Express **18**, 22283 (2010).
[17]M. Beruete, A. E. Serebryannikov, V. Torres, M. Navarro-Cía, and M. Sorolla, Appl. Phys. Lett. **99**, 154101 (2011).
[18]T. Xu and H. J. Lezec, Nat. Commun. **5**, 4141 (2014).
[19]S. Cakmakyapan, H. Caglayan, A. E. Serebryannikov, and E. Ozbay, Appl. Phys. Lett. **98**, 051103 (2011).
[20]A. E. Serebryannikov, E. Ozbay, and S. Nojima, Opt. Express **22**, 3075 (2014).
[21]P. Rodriguez-Ulibarri, M. Beruete, M. Navarro-Cía, and A. E. Serebryannikov, Phys. Rev. B **88**, 165137 (2013).
[22]M. Beruete, M. Sorolla, M. Navarro-Cía, F. Falcone, I. Campillo, and V. Lomakin, Opt. Express **15**, 1107 (2007).
[23]M. Beruete, M. Navarro-Cía, I. Campillo, P. Goy, and M. Sorolla, IEEE Microwave Wireless Compon. Lett. **17**, 834 (2007).
[24]See supplementary material at http://dx.doi.org/10.1063/1.4908260 for the comparison between the nominal hybrid fishnet metamaterial-dielectric grating structure, and that with air gaps between fishnet layers, and for further results such as frequency cuts proving good forward transmission and forward-to-backward transmission contrast.